Discovery of FLT3 inhibitors for the treatment of acute myeloid leukemia

Grimm, S.H.

Chapter 2

Chemical proteomics enables cellular selectivity profiling of clinical FLT3 inhibitors*

Introduction

Acute myeloid leukemia (AML) is an aggressive form of blood cancer in elderly people with poor prognosis. In approximately 20-30% of AML patients an internal tandem duplication (ITD) in the juxtamembrane domain of the Fms-like tyrosine kinase 3 (FLT3) receptor has been identified as a driver mutation. This modification of the FLT3 gene results in growth factor independent proliferation of immature blasts cells, thereby fatally disrupting normal hematopoietic function.[1–4] For this reason, kinase inhibitors targeting FLT3 have been developed for the treatment of AML.[5] Several compounds, including sunitinib, quizartinib, crenolanib, gilteritinib and midostaurin (Figure 1), have been clinically tested in AML patients,[6,7] resulting in the recent approval, by the FDA, of midostaurin in combination with current treatment (cytarabine and daunorubicin).[8,9]

* The data presented in this chapter was gathered in collaboration with Eva van Rooden, Ruud Wijdeven, Laura de Paus, Hengyi You, Marjolein Quik, Tom van der Wel, Elliot D. Mock, Hermen S. Overkleeft, Jacques Neefjes and Mario van der Stelt.

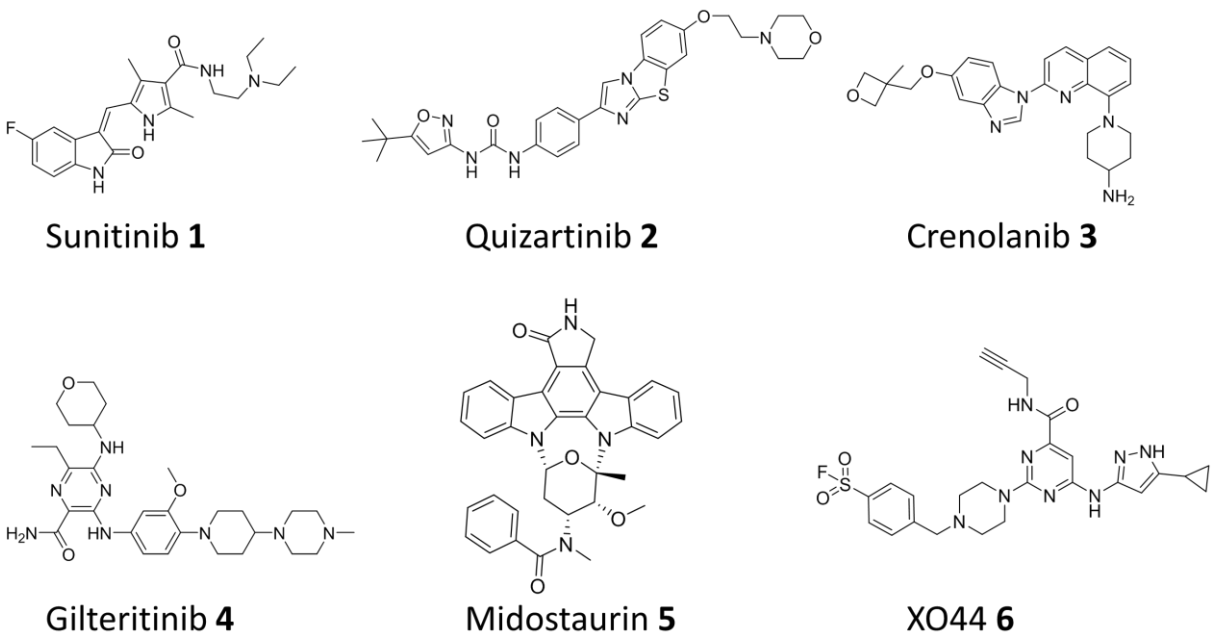

Figure 1: Chemical structures of the used compounds.

Most kinase inhibitors interact with the structurally and functionally conserved ATP-binding site, which is present in all 518 canonical human protein kinases. It is well-established that kinase inhibitors bind multiple proteins, and that this may affect their efficacy and toxicity.[10] Detailed investigation of the target-interaction landscape of kinase inhibitors is, therefore, important to understand their cellular and molecular mode of action. To this end, binding and activity assays with purified (recombinant) kinases or their catalytic domains are widely applied, however these assays do not recapitulate the cellular environment in which post-translational modifications, endogenous ligands, substrate levels, and protein-protein interactions may alter enzyme activity.[11–13] To address this issue, chemical proteomics methods have recently been developed to study target engagement in complex native (cellular) environments. These mass spectrometry (MS)-based assays make use of reversible bead-immobilized kinase inhibitors,[14] irreversible ATP-biotin probes,[15] photoaffinity-based probes,[16] or an irreversible pan-kinase probe (XO44, Figure 1).[12] The MS-based studies capture endogenously expressed kinases from complex, native proteomes and using inhibitors in competition experiments can be used to generate an off-target profile. For example, XO44, a fluorosulfonyl-based probe that covalently and irreversibly reacts with a conserved lysine-omega-amine, allowed the identification of 133 different kinases in Jurkat cells and was used to map the cellular target-interaction landscape of the approved drug dasatinib.[12]

The selectivity profile of the clinical FLT3 inhibitors has previously been investigated using binding-, activity- and Kinobeads-assays,[10,14] but the cellular target interaction profile has not been defined. This chapter reports the cellular target engagement landscape of five different FLT3 inhibitors (sunitinib, quizartinib, crenolanib, gilteritinib and midostaurin) in MV4-11 cells, a widely used cellular model for AML that harbors the FLT3-ITD mutant, and the lymphoma cell line U937. A recently, in-house developed label-free chemical proteomics protocol was

employed in which data-independent acquisition and ion mobility separation was used to increase peptide identification and the number of samples analyzed in the same experiment.[17]

Results

First, the activity of sunitinib, quizartinib, crenolanib, gilteritinib and midostaurin was confirmed in a biochemical assay using commercially available purified recombinantly expressed human FLT3 with a time-resolved fluorescence resonance energy transfer assay. All five inhibitors demonstrated strong inhibition with a half maximum inhibitory concentration (IC_{50}) in the low to sub-nanomolar range (Table 1). Crenolanib appeared to be the most potent inhibitor (pIC_{50} = 9.60 ± 0.07), whereas quizartinib the weakest inhibitor (pIC_{50} = 8.30 ± 0.07) in our assay. To determine the cellular activity of the clinical compounds, a cell proliferation assay using the FLT3-dependent AML cell line MV4-11, and as a control, the histiocytic lymphoma cell line (that is not dependent on FLT3 activity) U937 was performed (Table 1). All five inhibitors inhibited MV4-11 proliferation with nanomolar potency (pIC_{50}: 7.7 – 8.5), whereas the U937 cells were not sensitive to the inhibitors ($pIC_{50} \leq 5.5$), except for the pan-kinase inhibitor midostaurin (pIC_{50} = 6.85 ± 0.06). Altogether, these results confirm that the five compounds are potent, cellularly active FLT3 inhibitors inhibiting the growth of AML cells.

Table 1: Summary of pIC_{50} ± SEM *in vitro* (FLT3) and cellular (MV4-11 and U937).

	Sunitinib	**Quizartinib**	**Crenolanib**	**Gilteritinib**	**Midostaurin**	**XO44**
	1	**2**	**3**	**4**	**5**	**6**
pIC50 FLT3	9.01 ± 0.10	8.30 ± 0.07	9.60 ± 0.07	8.55 ± 0.07	8.84 ± 0.10	7.98 ± 0.11
pIC50 MV4-11	7.78 ± 0.04	8.55 ± 0.06	7.84 ± 0.07	7.81 ± 0.07	8.06 ± 0.04	6.90 ± 0.05
pIC50 U937	< 5	5.55 ± 0.13	< 5	5.10 ± 0.12	6.85 ± 0.06	n.a.

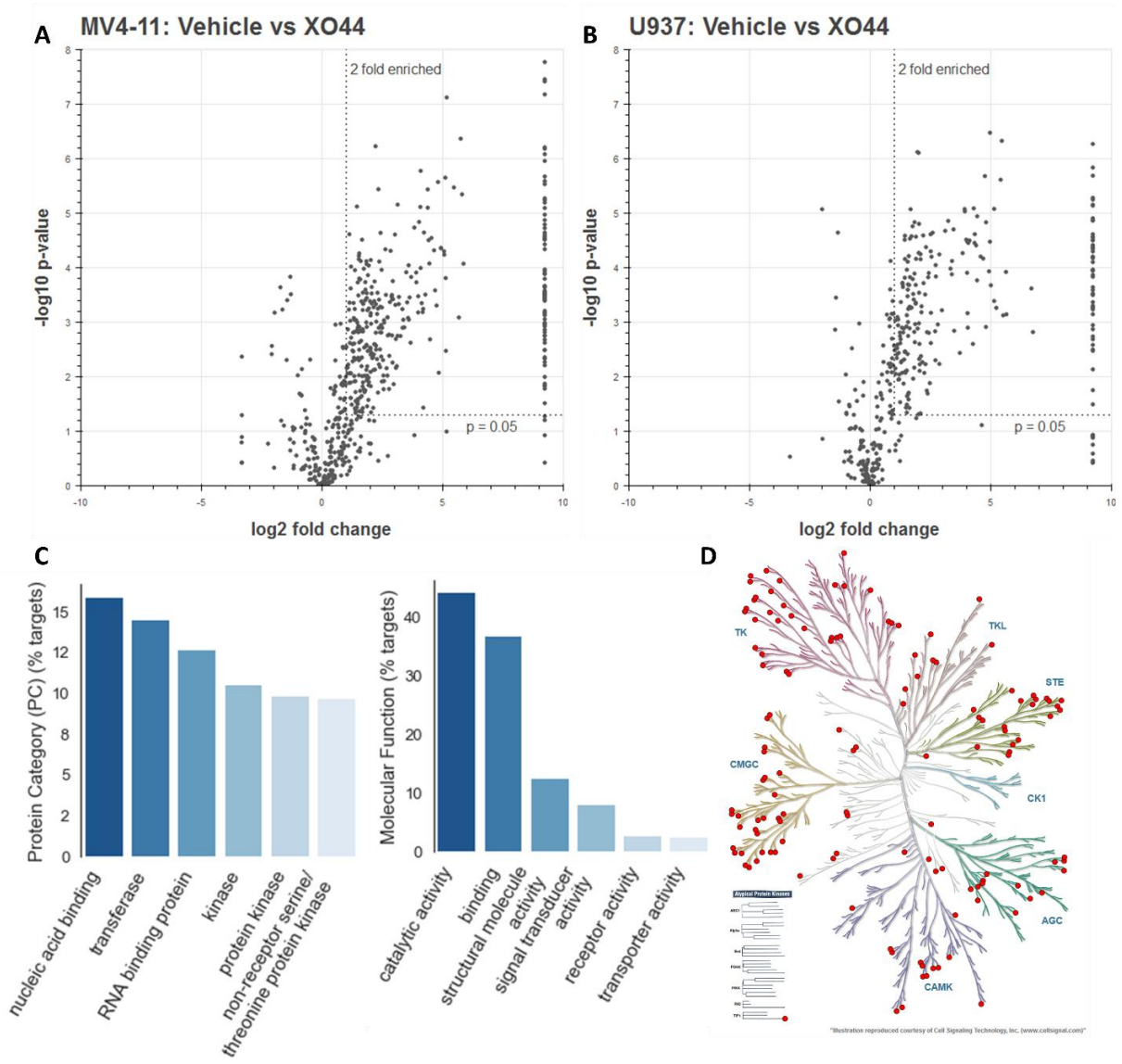

Figure 2: Analysis of the identified targets of XO44 in MV4-11 and U937 cells at 1 µM XO44. (A/B) Volcano plot of the label-free quantification signal from IsoQuant, vehicle vs XO44 treated MV4-11 and U937 cells. To enable plotting of all identified targets, infinite fold change (XO44 treated divided by vehicle control) was set to 600 and a fold change value of 0 was set to 0.1. Proteins are named targets of XO44, if there was a > 2-fold enrichment of quantification value, the probability associated with a Student's t-test (two-tailed distribution; two-sample equal variance) was < 0.05 and the conditions for the Benjamini–Hochberg correction with an FDR of 10% were fulfilled. (C) Targets found were analyzed by gene ontology using the panther protein-classification system (www.pantherdb.com). (D) From the targets of XO44, target kinases were selected according to annotations in Uniprot (transfer of P containing group (EC number Filter "2.7.-.-"). 147 unique kinases could be identified and were plotted on the canonical kinome-tree (13 targets could not be placed). (Illustration reproduced courtesy of Cell Signaling Technology, Inc. (www.cellsignal.com))

To determine the selectivity profile of the inhibitors in MV4-11 and U937 cells, a chemical proteomics experiment using XO44 as a cell-permeable pan-kinase probe was performed. To this end, XO44 was synthesized according to previously reported procedures (See experimental part for synthesis and chemical analysis).[12] MV4-11 and U937 cells (7 x 10^6 cells/mL) were incubated with 1 µM XO44 or vehicle (DMSO) for 30 min, subsequently lysed

and subjected to a Cu(I)-catalyzed alkyne-azide [2+3] cycloaddition ("click"-reaction) with a biotin-azide.[18] Probe targets were enriched via pull-down with avidin-agarose beads and digested with trypsin. The resulting peptides were analyzed by LC-MS/MS and quantified using PLGS and IsoQuant software. Probe targets were selected using a > 2-fold enrichment of quantification value, depending on whether the probability associated with a Student's t-test (two-tailed distribution; two-sample equal variance) was < 0.05 testing positive control versus negative control samples and the conditions for the Benjamini–Hochberg correction with an FDR of 10% were fulfilled (Figure 2A/B). Kinase targets were selected from this according to annotations in Uniprot (transfer of P containing group (EC number Filter "2.7.-.-"). In total 114 and 118 kinases were identified in MV4-11 and U937 cells, respectively. 150 unique kinases could be identified and 82 kinases were identified in both cell lines. Proteins from all kinase sub-families were identified (Figure 2D). Peptides derived from FLT3-ITD were identified, albeit just below the quantification limit using the standard statistical parameters, therefore the presence of the FLT3-ITD construct in MV4-11 cells was confirmed using genomic polymerase chain reaction (PCR) (SI). Furthermore, 415 non-kinase proteins, including ATP-binding proteins ATP-dependent RNA helicase DDX3Y, ADP/ATP translocase 2 and ATP synthase subunit alpha (mitochondrial), were also identified as probe targets. All targets were analyzed by gene ontology using the panther protein-classification system (www.pantherdb.com) (Figure 2C).

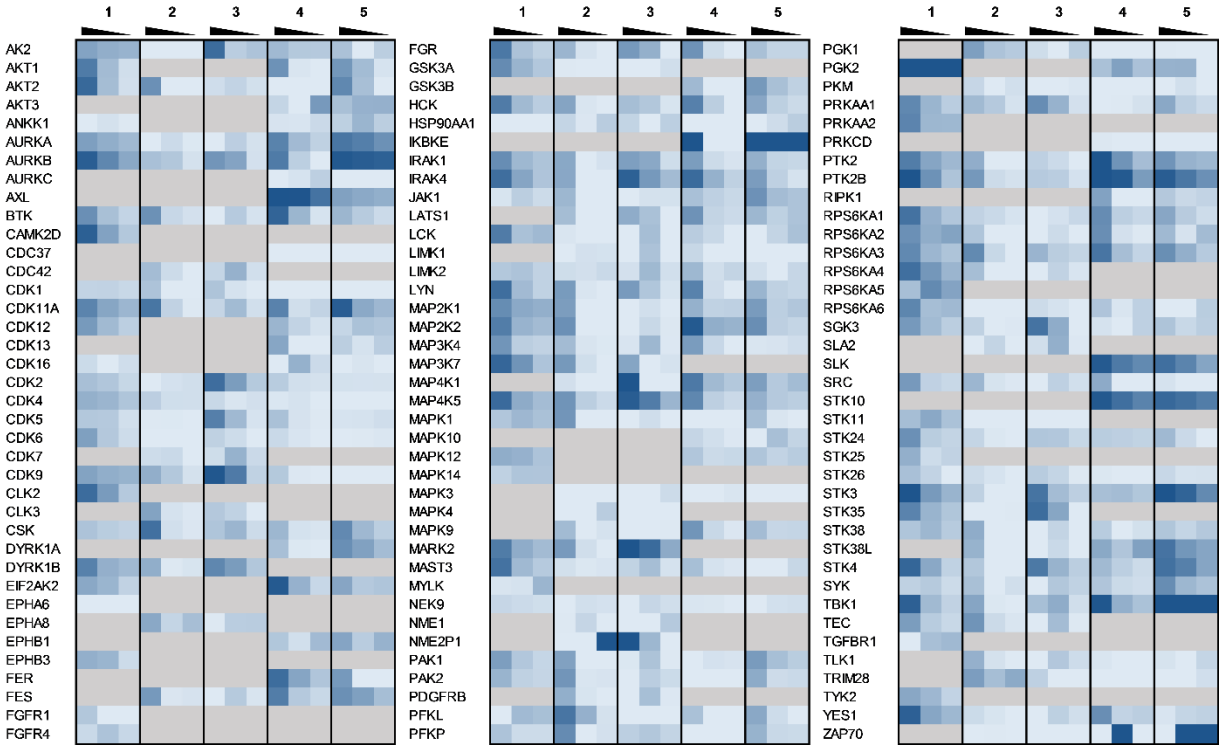

Figure 3: Heatmap of kinase inhibitor (**1** – **5**) targets in MV4-11. Kinase Targets were selected as described earlier. The heatmap shows the ratio of label free quantification signal from IsoQuant of inhibitor pretreated samples at three concentrations (100, 10 and 1 µM), normalized by only XO44 treatment after subtraction of negative control signal (e.g. 1: no difference in competitor and probe treated sample (light blue) 0: full competition of probe by the inhibitor (dark blue)).

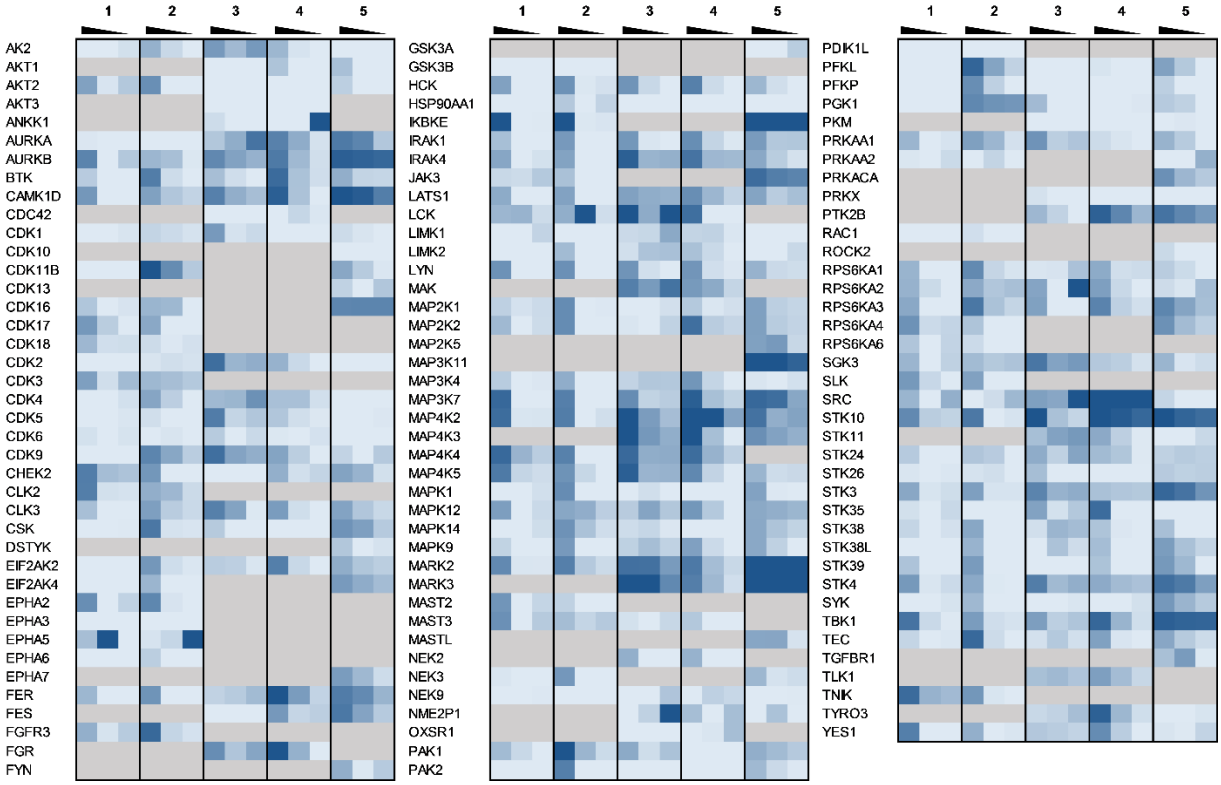

Figure 4: Heatmap of kinase inhibitor (**1** – **5**) targets in U937. Kinase Targets were selected as described earlier. The heatmap shows the ratio of label free quantification signal from IsoQuant of inhibitor pretreated samples at three concentrations (100, 10 and 1 µM), normalized by only XO44 treatment after subtraction of negative control signal (e.g. 1: no difference in competitor and probe treated sample (light blue) 0: full competition of probe by the inhibitor (dark blue)).

Next, the five clinical FLT3 inhibitors were tested at 1, 10 and 100 µM in a competitive chemical proteomics format using a 60 min pre-incubation-time before XO44 was added to MV4-11 or U937 cells for 30 min. These concentrations were chosen to represent 10x the IC_{50}-values (maximal efficacy) observed in the cellular proliferation assays. Kinases displaying > 50% reduction in probe labeling in a dose-dependent manner were designated as drug-inhibited targets. All targets for the five compounds in each cell line are summarized as heat maps in Figure 3 and Figure 4, as well as plotted as volcano-plots (SI Figure 1). Sunitinib and quizartinib were the most selective FLT3 inhibitors targeting PGK2 and PGK1 at 1 µM, respectively and in a dose-dependent fashion (SI). Crenolanib, gilteritinib and midostaurin were less selective and inhibited 12, 7, and 14 kinases at 1 µM in a dose-dependent fashion in MV4-11 and U937 cells (Table 2) respectively. Our data is in line with previously reported binding assays for midostaurin and sunitinib as reported in the ChEMBL database (SI).[19] Of note, at 1 µM midostaurin, a concentration that blocks the growth of both MV4-11 and U937 cells, AURKA, AURKB, IKBKE, PTK2B, STK3, STK10 and TBK1 were highly engaged in both cell lines. In U937 cells and at 10x IC_{50}-values, the compounds were significantly less selective (Table 2). At this high concentration, the clinical compounds inhibited 24 up to 39 kinases. TBK1, STK10, MAP4K2, MARK2 and MAP3K7 were inhibited by all clinical inhibitors at least at one of the tested concentrations.

Table 2: Summary of the identified targets for the corresponding inhibitors (**1** – **5**) at 10x IC50 on cell proliferation. Targets are selected if 50% outcompeted compared to 1 µM probe treatment without competitor.

1 µM in MV4-11 and U937 (10x IC_{50})

1		2		3		4		5	
MV4-11	**U937**	**MV4-11**	**U937**	**MV4-11**	**U937**	**MV4-11**	**U937**	**MV4-11**	**U937**
PGK2		NME2P1	PGK1		AK2	AKT3	STK10	AURKA	JAK3
			EPHA5		MAK	AXL	SRC	AURKB	TBK1
					SGK3	PTK2B	ANKK1	IKBKE	STK3
					MARK2	SLK		PTK2B	MAP3K11
					CDK4	STK10		STK10	CDK16
					SRC			STK3	STK10
					STK11			TBK	PTK2B
					LCK			ZAP70	AURKB
					RPS6KA2				CAMK1D
					MARK3				MARK3
					NME2P1				MARK2
					AURKA				IKBKE

100 µM in U937 (10x IC_{50})

1		2		3		4		5	
AURKB	MAP4K5	AKT2	MAP4K4	AK2	MAP3K7	ANKK1	MAP3K4	AURKA	MAP4K3
CAMK1D	MAPK12	BTK	MAP4K5	AURKA	MAP4K2	AURKA	MAP3K7	AURKB	MARK2
CDK17	MARK2	CDK11B	MAPK1	AURKB	MAP4K3	AURKB	MAP4K2	CAMK1D	MARK3
CHEK2	MAST2	CDK9	MAPK14	CAMK1D	MAP4K4	BTK	MAP4K3	CDK16	PRKACA
CLK2	MAST3	CHEK2	MAPK9	CDK1	MAP4K5	CAMK1D	MAP4K4	CSK	PTK2B
EPHA2	RPS6KA4	CSK	MARK2	CDK2	MARK2	CLK3	MAP4K5	EIF2AK4	RPS6KA3
EPHA5	SLK	EIF2AK2	NEK3	CDK4	MARK3	EIF2AK2	MAPK12	EPHA7	RPS6KA4
IKBKE	STK10	EPHA2	PAK1	CDK5	NME2P1	FER	MARK2	FER	STK10
LYN	STK4	EPHA5	PAK2	CDK9	PRKAA1	FES	MARK3	FES	STK3
MAP3K7	TBK1	FER	PFKL	CLK3	RPS6KA2	FGR	PTK2B	IKBKE	STK38L
MAP4K2	TNIK	FGFR3	PFKP	FGR	SGK3	HCK	RPS6KA3	IRAK1	STK39
MAP4K4	YES1	HCK	PGK1	HCK	SRC	IRAK1	SRC	JAK3	STK4
		IKBKE	RPS6KA1	IRAK1	STK10	IRAK4	STK10	MAP2K5	SYK
		IRAK1	RPS6KA3	IRAK4	STK11	LATS1	STK35	MAP3K11	TBK1
		LCK	STK10	LCK	STK3	LCK	TBK1	MAP3K7	TGFBR1
		LYN	STK39	LYN	STK4	LYN	TYRO3	MAP4K2	
		MAP2K1	TBK1	MAK	TBK1	MAK	YES1		
		MAP2K2	TEC			MAP2K2			
		MAP3K7	TNIK						
		MAP4K2							

Furthermore, several previously not reported targets could be identified, amongst them AK2, MAK and SGK3 for crenolanib, SRC, SLK and STK10 for gilteritinib, as well as CDK16 for midostaurin. All of these except AK2 were available to be tested at KinaseProfiler™ from Eurofins, where in a radiometric assay, residual protein activity was determined at 1 and 10 µM. The results from this study are shown in Table 3. All three gilteritinib targets (SRC, SLK and STK10) show full inhibition at 1 and 10 µM. Crenolanib and midostaurin show light (1 µM) and moderate (10 µM) inhibition towards their examined targets.

Table 3: Percent (%) residual kinase activity as tested in a radiometric assay at Eurofins KinaseProfiler™.

	Crenolanib			**Gilteritinib**			**Midostaurin**	
µM	**1**	**10**		**1**	**10**		**1**	**10**
MAK	99 ± 12	65 ± 3	**SRC**	3 ± 1	1 ± 0	**CDK16**	94 ± 1	55 ± 3
SGK3	89 ± 10	60 ± 8	**SLK**	-3 ± 1	-2 ± 1			
			STK10	2 ± 1	-1 ± 0			

Discussion

The determination of the cellular target interaction landscapes of experimental drugs is important to assess their safety profile and to guide their clinical development. Using activity-based proteomics this lab has previously mapped the cellular target interaction landscape of the drug BIA 10-2474 that killed a volunteer in a phase 1 study. BIA 10-2474 was a significantly more promiscuous lipase inhibitor in living human neuronal cells compared to its biochemical selectivity profile.[13] In the field of kinases, several methods, including cellular thermal shift assay (CETSA),[20] energy transfer assays (nano-BRET),[21] and chemical proteomics[12] have recently been developed and applied to map selectivity profiles of clinical compounds in live cells. The value of these techniques is that they capture cell permeability of the compound and take into account the physiological complexity of full-length kinases and their regulation by the native cellular environment. For example, most biochemical kinase selectivity panels operate at ATP concentrations close to the K_M (10-100 µM), whereas cellular ATP concentrations exceeds 1 mM in the nucleus and cytosol where kinases are active. This leads to a shift in potency for kinase engagement with ATP-competitive inhibitors, which alters their selectivity profile.

In the present study the cellular target engagement profile of five clinical FLT3 kinase inhibitors was determined using chemical proteomics. By using the chemical probe XO44 to covalently capture kinases in living MV4-11 and U937 cells, in combination with mass spectrometry-based detection, over 140 kinases were identified. Competitive activity-based proteomics assays were performed with sunitinib, quizartinib, crenolanib, gilteritinib and midostaurin, kinase inhibitors that are considered in the treatment of AML. As was also noted previously for dasatinib[12,21] and crizotinib,[21] the compounds displayed an improved selectivity profile in living cells compared to biochemical assays. The high cellular ATP levels likely

explains improved selectively. Alternatively, and despite choosing kinetically balanced conditions, it cannot be completely ruled out that the covalent XO44 out-competed the reversible inhibitors. Furthermore, kinases that are absent or have an expression level below the detection limit of our assay will also not be evaluated in the current setup. The inclusion of multiple different cell lines and development of new broad-spectrum activity-based probes with a different target kinase profile may improve the coverage of the kinome.

Ideally, the identified target-ligand interaction profiles should be validated by orthogonal techniques.[13,17,22] Indeed, many cellular off-targets were previously identified in biochemical assays (for instance 12 out of 14 targets for midostaurin are listed in the ChEMBL database).[23] MARK2 and MARK3 were confirmed as targets for crenolanib,[14] while AXL and PTK2B were previously reported as targets for gilteritinib. In fact, gilteritinib is being developed as a dual FLT3/AXL inhibitor.[24] In contrast, it was previously reported that crenolanib is not active against LCK,[14] which might indicate that LCK is a false negative hit or that cellular regulation of LCK activity is required to observe the effect of crenolanib. Furthermore, unprecedented off-targets were also identified by the chemical proteomics assay, such as CDK16 for midostaurin, SRC, SLK and STK10 for gilteritinib and AK2, MAK and SGK3 for crenolanib. Of interest, AK2 plays a central role in hematopoiesis[25] and biallelic mutations in AK2 cause a strong decrease in protein expression and results in reticular dysgenesis, which might make AK2 an undesirable off-target.[26] Of these newly described targets, SRC, SLK and STK10 could be confirmed as targets of gilteritinib and partial inhibition of CDK16 (midostaurin) as well as MAK and SGK3 (crenolanib) in an orthogonal *in vitro* assay could be shown. While some reported off-targets for the five kinase inhibitors tested can be confirmed, we also identified others, which will require further biological validation. Especially the inhibition of AK2 by crenolanib is of importance in view of its potential toxicological side-effects.

Of note, the off-target profile of the assessed inhibitors may provide additional information about their cellular mode of action that may even add to the anti-cancer effects observed. For example, AURKA and AURKB are inhibited by midostaurin in MV4-11 and U937 cells, but these kinases are also under investigation as potential therapeutic targets for hematological cancers.[27,28] This may suggest that they could contribute to the efficacy of midostaurin. It is important to understand the off-targets of the anti-AML kinase inhibitors, as these are now finding their way into the clinic. The off-targets can explain some of the clinical effects and side-effects observed in the treatment of patients with these drugs.

Experimental

In vitro FRET based FLT3 assay

In a 384-wells plate (PerkinElmer 384 Flat White), 5 µL kinase/peptide mix (0.06 ng/µL FLT3 (Life Technologies; PV3182; Lot: 1614759F), 200 nM peptide (PerkinElmer; Lance® Ultra ULightTM TK-peptide; TRFO127-M; Lot: 2178856)) in assay buffer (50 mM HEPES pH 7.5, 1 mM EGTA, 10 mM $MgCl_2$, 0.01% Tween-20, 2 mM DTT) was dispensed. Separately inhibitor solutions (10 µM – 0.1 pM) were prepared in assay buffer containing 400 µM ATP and 1% DMSO. 5 µL of these solutions were dispensed and the plate was incubated in the dark at room temperature. After 90 minutes the reaction was quenched by the addition of 10 µL of 20 mM EDTA containing 4 nM antibody (PerkinElmer; Lance® Eu-W1024-anti-phosphotyrosine(PT66); AD0068; Lot: 2342358). After mixing, samples were incubated for 60 minutes in the dark. The FRET fluorescence was measured on a Tecan Infinite M1000 Pro plate reader (excitation 320 nm, emission donor 615 nm, emission acceptor 665 nm). Data was processed using Microsoft Excel 2016, pIC_{50} values were fitted using GraphPad Prism 7.0. Final assay concentrations during reaction: 200 µM ATP, 0.03 ng/µL FLT3, 100 nM Lance TK-peptide, 0.5% DMSO. Compounds were tested in n=2 and N=2.

In situ testing of kinase inhibitors

Cell lines were obtained as a gift from Linda Smit (VUMC, Amsterdam, the Netherlands) and were tested on regular basis for mycoplasma contamination. To evaluate inhibitor effect on cell proliferation MV4-11 and U937 cells were grown in RPMI, supplemented with 10% fetal bovine serum in an incubator at 37°C under 5% CO_2 atmosphere. For viability assays, 10,000 cells were seeded per well in a 96-wells plate and inhibitors were added at the indicated concentration. After three days, cell viability was measured using the Cell Titer Blue viability assay (Promega) and fluorescence was measured using the Clariostar (BMG Labtech). Relative survival was normalized to the untreated control and corrected for background signal. Data was processed using Microsoft Excel 2016, pIC_{50} values were fitted using GraphPad Prism 7.0. Experiments were performed in either n=3 or n=2.

Genomic DNA extraction and PCR

U937 and MV4-11 cells (1 x 10^6) were harvested by centrifugation (1,000 g, 5 min). Medium was removed and cell pellet was suspended in 50 µL QuickExtract™ (Epicentre). Samples were incubated at 65°C for 6 min, mixed by vortexing and then incubated at 98°C for 2 min. Genomic DNA extracts were diluted in sterile water and directly used in PCR reactions. Genomic PCR reactions were performed on 5 µL isolated genomic DNA extract using Phusion High-Fidelity DNA Polymerase (Thermo Fisher) in Phusion HF buffer with 10 pmol primers (forward: GCAATTTAGGTATGAAAGCCAGC, reverse: CTTTCAGCATTTTGACGGCAACC) in a total volume of 50 µL. Amplicons were purified using NucleoSpin® Gel and PCR Clean-up kit (Macherey-Nagel) and analyzed by Sanger sequencing (Macrogen).[29]

Synthetic procedures

Solvents were purchased from Biosolve, Sigma Aldrich or Fluka and, if necessary dried over 3Å or 4Å molecular sieves. Reagents purchased from chemical suppliers were used without further purification, unless stated otherwise. O_2- or H_2O-sensitive reactions were performed under argon or nitrogen atmosphere and/or under exclusion of H_2O. Reactions were followed by thin layer chromatography and was performed using TLC Silica gel 60 F_{245} on aluminium

sheets, supplied by Merck. Compounds were visualized by UV absorption (254 nm) or spray reagent (permanganate (5 g/L $KMnO_4$, 25 g/L K_2CO_3)). TLCMS was measured on a thin layer chromatography-mass spectrometer (Advion, Eppression L CMS; Advion, Plate Express). ^1H and ^{13}C-NMR spectra were performed on one of the following Bruker spectrometers: DPX 300 NMR spectrometer (300 MHz), equipped with 5mm-BBO-z-gradient-probe; AV-400 NMR spectrometer (400 MHz), equipped with 5mm-BBO-z-gradient-probe; AV-500 NMR spectrometer (500 MHz), equipped with BBFO-z-gradient-probe; AV-600 NMR spectrometer (600 MHz), equipped with 5mm-Cryo-z-gradient probe. NMR spectra were measured in deuterated methanol, chloroform or DMSO and were referenced to the residual protonated solvent signals as internal standards (chloroform-*d* = 7.260 (^1H), 77.160 (^{13}C); methanol-d_4 = 3.310 (^1H), 49.000 (^{13}C); DMSO-d_6 = 2.500 (^1H), 39.520 (^{13}C)). Signals multiplicities are written as s (singlet), bs (broad singlet), d (doublet), t (triplet), q (quartet), p (pentet) or m (multiplet). Coupling constants (*J*) are given in Hz. Preparative HPLC (Waters, 515 HPLC pump M; Waters, 515 HPLC pump L; Waters, 2767 sample manager; Waters SFO System Fluidics Organizer; Waters Acquity Ultra Performance LC, SQ Detector; Waters Binary Gradient Module) was performed on a Phenomenex Gemini column (5 µM C18, 150 x 4.6 mm) or a Waters XBridgeTM column (5 µM C18, 150 x 19 mm). Diode detection was done between 210 and 600 nm. Gradient: ACN in (H_2O + 0.2% TFA). HRMS (Thermo, Finnigan LTQ Orbitrap; Thermo, Finnigan LTQ Pump; Thermo, Finnigan Surveyor MS Pump PLUS Thermo, Finnigan Surveyor Autosampler; NESLAB, Merlin M25). Data acquired through direct injection of 1 mM of the sample in ACN/H_2O/*t*-BuOH (1:1:1), with mass spectrometer equipped with an electrospray ion source in positive mode (source voltage 3.5 kV, sheath gas low 10, capillary temperature 275°C) with resolution R = 60.000 at m/z = 400 (mass range = 150-2000) and dioctylphtalate (m/z = 391.28428) as lock mass. Gradient: ACN in (H_2O + 0.1% TFA). All tested compounds were checked for purity by LCMS liquid chromatography-mass spectrometer, either on a Thermo (Thermo Finnigan LCQ Advantage Max; Thermo Finnigan Surveyor LC-pump Plus; Thermo Finnigan Surveyor Autosampler Plus; Thermo Finnigan Surveyor PDA Plus Detector; Phenomenex Gemini column (5 µm C18, 50 x 4.6 mm)) or a Waters (Waters 515 HPLC pump M; Waters 515 HPLC pump L; Waters 2767 sample manager; Waters SFO System Fluidics Organizer; Waters Acquity Ultra Performance LC, SQ Detector; Waters binary gradient module; Phenomenex Gemini column (5 µm C18, 150 x 4.6 mm)) system and were determined to be >95% pure by integrating UV intensity recorded.

2,6-Dichloropyrimidine-4-carbonyl chloride (7)

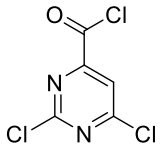

A round-bottom flask was charged with orotic acid (15.6 g, 100 mmol, 1 eq) dissolved in phosphorus oxychloride (46 mL, 500 mmol, 5 eq) and 10 drops DMF. After stirring at reflux for 19 h, *n*-hexane (250 mL) was added, the mixture was stirred vigorously for 10 min and transferred into a separator funnel containing H_2O (100 mL). The layers were separated and the organic layer was washed with brine (1x100 mL), dried over $MgSO_4$ and concentrated under reduced pressure to yield the product (12.8 g, 60%) which was used without further purification. ^1H NMR (500 MHz, chloroform-*d*) δ 8.00 (s, 1H). ^{13}C NMR (126 MHz, chloroform-*d*) δ 167.17, 165.27, 161.56, 158.19, 119.70.

2,6-Dichloro-*N*-(prop-2-yn-1-yl)pyrimidine-4-carboxamide (8)

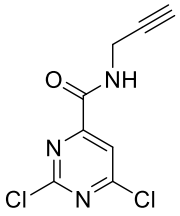

A round-bottom flask was charged with 2,6-dichloropyrimidine-4-carbonyl chloride (7) (1.15 g, 5 mmol, 1 eq) dissolved in dry DCM (50 mL) was cooled to -78°C. After addition of Et_3N (0.91 mL, 6.5 mmol, 1.3 eq) and dropwise addition of propargyl amine (0.33 mL, 5.15 mmol, 1 eq), the mixture was stirred for 3.5 h, quenched by addition of H_2O (50 mL) and diluted with DCM (60 mL). The phases were separated and the organic layer was washed with H_2O (1x50 mL) and brine (1x75 mL), dried over Na_2SO_4, filtered and concentrated under reduced pressure. The resulting crude product was purified via flash-column chromatography (SiO_2, 5% → 50% EtOAc in pentane) to yield the product (0.88 g, 76%). ^{1}H NMR (500 MHz, methanol-d_4) δ 8.09 (s, 1H), 4.21 (d, *J* = 2.6 Hz, 2H), 2.57 (t, *J* = 2.5 Hz, 1H). ^{13}C NMR (126 MHz, methanol-d_4) δ 165.41, 161.59, 161.40, 160.68, 119.26, 79.76, 72.40, 29.71.

2-Chloro-6-((5-cyclopropyl-1*H*-pyrazol-3-yl)amino)-*N*-(prop-2-yn-1-yl)pyrimidine -4-carboxamide (9)

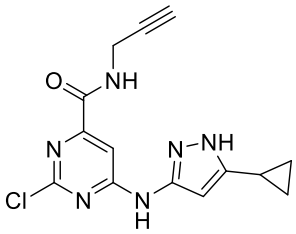

A vial was charged with 2,6-dichloro-*N*-(prop-2-yn-1-yl)pyrimidine-4-carboxamide (8) (229 mg, 1.00 mmol, 1 eq), 5-cyclopropyl-1*H*-pyrazol-3-amine (138 mg, 1.12 mmol, 1.1 eq), DIPEA (0.2 mL, 1.15 mmol, 1.15 eq) dissolved in THF (2 mL). After stirring for 45 h at RT, the mixture was diluted with methanol and concentrated onto celite. The crude product was purified via flash-column chromatography (SiO_2, dry-loading, 50% → 80% EtOAc in pentane) to yield the product (111 mg, 35%). ^{1}H NMR (400 MHz, methanol-d_4) δ 7.47 (bs, 1H), 6.28 (bs, 1H), 4.14 (d, *J* = 2.5 Hz, 2H), 2.61 (t, *J* = 2.5 Hz, 1H), 1.97 – 1.85 (m, 1H), 1.08 – 0.94 (m, 2H), 0.78 – 0.71 (m, 2H). ^{13}C NMR (101 MHz, methanol-d_4) δ 164.28, 161.22, 148.48, 94.65, 80.13, 72.28, 30.76, 29.61, 8.25, 7.65. LCMS (ESI, Thermo, C_{18}, linear gradient, 10% → 90% ACN in H_2O, 0.1% TFA, 10.5 min): t_R = 5.76 min; *m/z* : 317 $[M+1]^+$.

***tert*-Butyl piperazine-1-carboxylate (10)**

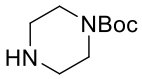

A round bottom flask was charged with *n*-butanol (45 mL), 2 M aqueous NaOH (7.5 mL) and piperazine (3.17 g, 14.5 mmol, 1 eq). After dropwise addition of Boc_2O (3.16 g, 36.7 mmol, 2.5 eq) dissolved in *n*-butanol (5 mL), the mixture was stirred for 60 min at RT and then concentrated under reduced pressure. H_2O (10 mL) was added and di-substituted piperazine was removed by filtration. The filtrate was extracted with DCM (3x30mL) and the combined organic layers were dried over Na_2SO_4 and concentrated under reduced pressure to yield the product (1.96 g, 73%) without further purification. ^{1}H NMR (500 MHz, methanol-d_4) δ 3.39 (bs, 4H), 2.81 – 2.70 (m, 4H), 1.46 (s, 9H). ^{13}C NMR (126 MHz, methanol-d_4) δ 156.34, 81.15, 45.89, 44.71, 28.68.

tert-Butyl 4-(4-((5-cyclopropyl-1_H_-pyrazol-3-yl)amino)-6-(prop-2-yn-1-ylcarbamoyl) pyrimidin-2-yl) piperazine-1-carboxylate (11)

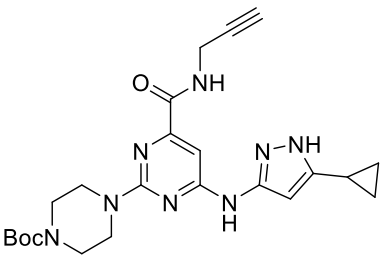

A vial was charged with 2-chloro-6-((5-cyclopropyl-1*H*-pyrazol-3-yl)amino)-*N*-(prop-2-yn-1-yl)pyrimidine -4-carboxamide (9) (96 mg, 0.30 mmol, 1 eq), *tert*-butyl piperazine-1-carboxylate (10) (78 mg, 0.42 mmol, 1.4 eq) and DIPEA (0.13 mL, 0.76 mmol, 2.5 eq) dissolved in *n*-butanol (2.5 mL). After stirring for 11 h at 100°C, the mixture was diluted with methanol and concentrated onto celite. The crude product was purified via flash-column chromatography (SiO_2, dry-loading, 30% → 70% EtOAc in pentane) to yield the product (168 mg, quant.). ^{1}H NMR (500 MHz, methanol-d_4) δ 6.83 (bs, 1H), 6.09 (bs, 1H), 4.14 (d, *J* = 2.5 Hz, 2H), 3.86 – 3.81 (m, 4H), 3.50 (bs, 4H), 2.59 (t, *J* = 2.5 Hz, 1H), 1.93 – 1.86 (m, 1H), 1.49 (s, 9H), 1.03 – 0.95 (m, 2H), 0.76 – 0.71 (m, 2H). ^{13}C NMR (126 MHz, methanol-d_4) δ 166.37, 163.33, 162.52, 157.81, 157.28, 156.56, 156.37, 95.01, 94.65, 81.42, 80.63, 71.96, 44.90, 44.18, 29.46, 28.68, 8.27, 7.72. LCMS (ESI, Thermo, C_{18}, linear gradient, 10% → 90% ACN in H_2O, 0.1% TFA, 10.5 min): t_R = 6.41 min; *m/z* : 467 $[M+1]^+$.

4-((4-(4-((5-Cyclopropyl-1_H_-pyrazol-3-yl)amino)-6-(prop-2-yn-1-ylcarbamoyl) pyrimidin-2-yl)piperazin-1-yl)methyl)benzenesulfonyl fluoride (6, XO44)

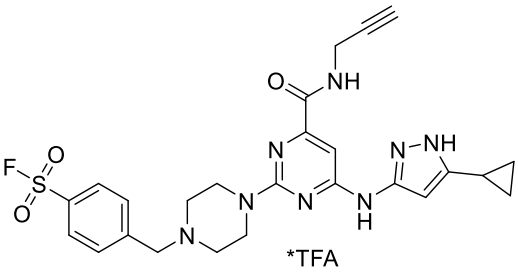

Step 1: *tert*-butyl 4-(4-((5-cyclopropyl-1*H*-pyrazol-3-yl)amino)-6-(prop-2-yn-1-ylcarbamoyl) pyrimidin-2-yl)piperazine-1-carboxylate (11) (168 mg, 0.46 mmol, 1 eq) was dissolved in chloroform (8 mL) and TFA (2 mL). After stirring the mixture for 75 min, it was concentrated under reduced pressure. The resulting crude product was used in Step 2 without further purification.

Step 2: A vial was charged with crude product from Step 1 (109 mg, 0.30 mmol, 1 eq), 4-(bromomethyl)benzenesulfonyl fluoride (140 mg, 0.55 mmol, 1.8 eq) and DIPEA (0.13 mL, 0.75 mmol, 2.5 eq) dissolved in DMF (1 mL) and DCM (4 mL). The resulting mixture was stirred at RT for 80 min and concentrated under reduced pressure. The residue was redissolved in EtOAc (20 mL) and washed with saturated aqueous Na_2CO_3 (1x20 mL), dried over Na_2SO_4, filtered and concentrated under reduced pressure. The resulting crude product was purified by preparative HPLC (Gemini C_{18}, 25% → 35% ACN in H_2O 0.2% TFA, 10 min gradient) to yield the product as a TFA salt after lyophilisation (58 mg, 30%). ^{1}H NMR (500 MHz, methanol-d_4) δ 8.23 (d, *J* = 8.4 Hz, 2H), 7.91 (d, *J* = 8.4 Hz, 2H), 6.96 (s, 1H), 6.04 (s, 1H), 4.55 (s, 2H), 4.14 (d, *J* = 2.5 Hz, 2H), 4.08 (bs, 4H), 3.39 (bs, 4H), 2.60 (t, *J* = 2.5 Hz, 1H), 1.96 – 1.89 (m, 1H), 1.03 – 0.98 (m, 2H), 0.77 – 0.72 (m, 2H). ^{13}C NMR (126 MHz, DMSO-d_6) δ 163.50, 161.31, 160.35, 156.12, 147.08, 138.33, 133.41, 132.77 (d, *J* = 23.9 Hz), 129.09, 128.12 (d, *J* = 92.3 Hz), 95.36, 93.03, 81.29, 72.82, 58.10, 51.02, 40.90, 28.34, 8.24, 7.13. LCMS (ESI, Thermo, C_{18}, linear gradient, 10% → 90% ACN in H_2O, 0.1% TFA, 10.5 min): t_R = 8.27 min; *m/z* : 539 $[M+1]^+$. HRMS calculated for $C_{25}H_{28}FN_8O_3S$ 539.19836 $[M+1]^+$, found 539.19822.

Chemical proteomics assay protocol

The assay protocol is adapted from an earlier publication.[17]

Preparation of Reagents and Stocks

Acetonitrile(ACN): ULC/MS grade (Biosolve, cat. no. 012041)

Chloroform($CHCl_3$): (Sigma, cat. no. 32211-M)

DMSO: (Sigma, cat. no. 34943-M)

Formic acid(FA): LC-MS grade (Actuall Chemicals, art. nr. 8060128A1)

Methanol: Reagent grade (Sigma, cat. no. 32213-M) or ULC/MS grade (Biosolve, cat. no. 136841)

Pierce™ Avidin Agarose: (Thermo Scientific, cat. no. 20219 20225)

Benzonase stock: Dilute benzonase nuclease (Santa Cruz Biotechnology, cat. no. sc-202391) to 10 U/µL. Store at -20℃.

$CaCl_2$ stock: Dissolve 147 mg calcium chloride dihydrate ($CaCl_2 \cdot 2\ H_2O$; Merck Millipore, cat. no. 102382) in 1 mL water to prepare a 1M $CaCl_2$ solution. Store the stock at room temperature.

DTT stock: Dissolve 1.54 g dithiothreitol (DTT; BioChemica, cat. no A1101) in water to a final volume of 10 mL for a 1M solution. Aliquots can be stored at -20 °C for up to 3 months.

IAA stock: Dissolve 92 mg iodoacetamide (IAA; Sigma, cat. no. I6125) in 1 mL water for a final concentration of 0.5 M. Light-sensitive. Prepare directly before use.

$MgCl_2$ stock: Dissolve 2.0 g of magnesium chloride hexahydrate ($MgCl_2 \cdot 6\ H_2O$; Acros Organics, cat. no. 413415000) in water to a final volume of 10 mL for a 1 M solution. Store the stock at room temperature.

NaCl stock: Dissolve 0.58 g of sodium chloride (NaCl; Chem-Lab, art. no. CL00.1423) in water to a final volume of 10 mL for a 1 M solution. Store the stock at room temperature.

NH_4HCO_3 buffer: Dissolve 198 mg ammonium bicarbonate (NH_4HCO_3; Fluka, cat. no. 09830) in water to a final volume of 10 mL for a 250 mM solution. Prepare directly before use.

PBS stock: Dilute 10x PBS solution ten times in Milli-Q water. Prepare the solution in a laminar hood. Store the stock at room temperature.

SDS stock: Prepare a 10% wt/vol sodium dodecyl sulfate (SDS; MP Biomedicals cat. no. 811032) solution in water. Store the stock at room temperature.

Tris stock: Prepare 1M tris(hydroxymethyl)aminomethane (Tris; Acros Organics cat. no. 16762) in water. Adjust pH to 8 with HCl. Store the stock at room temperature.

Trypsin solution: Dissolve 20 µg of trypsin (sequencing grade; Promega, cat. no. V5111) in 40 µL 1 mM HCl (hydrochloric acid; Sigma, cat. no. 30721-M) solution (diluting 37% HCl (~12 M) into water, pH=3) to get a final concentration of 0.5 µg/µL. Store at -20℃ and avoid freeze-thaw cycles.

Yeast enolase stock: Dissolve 1 nmol yeast enolase (Waters, product no. 186002325. SwissProt P00924) in 1 mL 3% acetonitrile in water (vol%).

Biotin-Azide: Dissolve solid biotin-azide (Cayman Chemical, product no. 13040, CAS: *908007-17-0*) in DMSO to reach a 4 mM concentration.

$CuSO_4$: Dissolve solid $CuSO_4(H_2O)_5$ in H_2O to reach a 100 mM concentration.

Na Ascorbate: Dissolve solid Na Ascorbate in H_2O to reach a 1 M concentration.

THPTA: Dissolve tris-hydroxypropyltriazolylmethylamine in DMSO to reach a 100 mM concentration.

Preparation of Mixes

- **LC-MS sample solution(2mL)**

0.1% (v/v) FA	2 µL	FA
3% (v/v) ACN	60 µL	ACN
97% (v/v) H_2O	1900 µL	MilliQ
20 fmol/µL enolase	40 µL	yeast enolase stock

Note: Prepare directly before use.

- **OB-Dig buffer(6mL)**

100 mM Tris	600 µL	Tris stock
100 mM NaCl	600 µL	NaCl stock
1 mM $CaCl_2$	6 µL	$CaCl_2$ stock
2% (v/v) ACN	120 µL	ACN

Note: Prepare directly before use

- **PBS/SDS**

0.5% (w/v) SDS	50 mL	SDS stock
99.5% (w/v) PBS	950 mL	PBS stock

Note: Prepare the solution in a laminar hood. Add SDS stock in the end. Store the stock at room temperature.

- **Stage tip solution A(100mL)**

0.5%(v/v) FA	500 µL	FA
99.5% (v/v) H_2O	100 mL	MilliQ

- **Stage tip solution B(100mL)**

0.5%(v/v) FA	500 µL	FA
80%(v/v) ACN	80 mL	ACN
20%(v/v) H_2O	20 mL	MilliQ

- **Urea buffer (10 mL)**

6M urea	3.6 g	Urea, Sigma, cat. no. 33247
25mM NH_4HCO_3	1 mL	NH_4HCO_3 buffer
In water	10 mL	MilliQ

Note: Prepare directly before use.

Cell treatment

Incubation

MV4-11 or U937 cells were cultured in IMDM or RPMI1640 (Sigma Aldrich) supplemented with stable glutamine and phenolred (PAA), 10% new born calf serum or 10% fetal calf serum (Biowest), penicillin and streptomycin at 37°C with 5% CO_2. Cell passage was performed every 2-3 days, growing these suspension cells at 2-10x10^5 cells/mL in 50 mL medium.

1) Count the cells: mix the cell suspension homogenously with a 25 mL pipette. Then take 3 mL cell suspension from the cell culture flask and transfer to 15 mL centrifuge tube. Mix 10 µL cell suspension from the centrifuge tube with 10 µL trypan blue. Pipette 10 µL of the mixture into a counting chamber. Count live/dead cells using a Biorad TC10 cell counter. Make sure to gently vortex the tube before counting.
2) Collect enough cell solution in a 50 mL centrifuge tube to obtain a final amount of 7×10^6 cells per sample. Collect the cells by centrifugation (10 min, 300 g) and discard the supernatant.
3) Add serum-free medium to the centrifuge tube and re-suspend the cell pellet gently with a 25 mL pipette to reach a final concentration of 7×10^6 cells/mL.
4) Add 1 mL of cell solution per sample to 1.5 mL Eppendorf tubes.

Note: To minimize the sample difference between samples, first add 500 µL from the first one to the last one. Then gently vortex the centrifuge tubes and put it upside down to homogenize the cell solution. Then add the other 500 µL cell solution from the last one to the first one.

5) Add 10 µL of DMSO or inhibitor (pre-diluted in DMSO to reach the desired final concentration) depending on the condition. Each condition should be tested in triplicate. Of note, one positive control replicate in kinase17_raw had to excluded due to large parts of the sample being lost during chloroform/methanol precipitation.
6) Puncture a hole with a needle on a new Eppendorf cap and install this cap to the original Eppendorf.
7) Start the first incubation at 37°C with 5% of CO_2 for 60 min.
8) Add 1 µL of DMSO or probe depending on the condition. Start second incubation at 37°C with 5% of CO_2 for 30 min.
9) Harvest cells by centrifuging the samples (10 min, 300 g). Remove the supernatant with vacuum suction device with a yellow pipette tip at its tip.
10) Snap freeze the pellet in liquid nitrogen.

Cell lysis

11) Thaw the samples on ice.
12) Dilute benzonase solution to 25 U/mL in MilliQ.
13) Add 225 µL benzonase solution to each sample and lyse cells by pipetting up and down with a 200 µL pipet until all the pellet is gone. Incubate on ice for 10 min.

14) Continue lysis by adding 25 µL 10% SDS solution to the samples (resulting in a concentration of 1% SDS in the sample). Incubate the samples at 95°C for 5 min. Spin down shortly when the samples cool down to room temperature.

Click reaction

15) Prepare 25 µL click mix per sample according to the list:

Reagents, Stock Conc.	Dilution factor	Volume (µL)
$CuSO_4 \cdot 5H_2O$, 100 mM	10×	2.5
Na Ascorbate, 1 M	17.86×	1.4
THPTA, 100 mM	50×	0.5
Biotin-Azide, 4 mM	10×	2.5
Milli Q water		18.1
	Total	25

Add the reagent according to the order on the list. Vortex gently after each reagent. The final color should be lightly yellow-golden.

16) Add 25 µL click mix to each sample. Incubate at 37°C while shaking (300 rpm) for 1 h, followed by a short centrifugation.

Methanol/chloroform precipitation

17) Add 225 µL Milli Q water to each sample for a final volume of 500 µL.

18) Add 666 µL MeOH and vortex.

19) Add 166 µL $CHCl_3$ and vortex.

20) Add 150 µL water and vortex; this should result in a cloudy suspension.

21) Pellet the precipitated protein by centrifugation (10 min, 1500 g), this should result in a floating pellet.

22) Remove the upper and lower layer without disturbing pellet (this works best by holding the tube at the angle of 45° to stick the protein pellet against the side).

23) Add 600 µL MeOH to the pellet.

24) Resuspend the pellet by sonication with a probe sonicator (10 sec, 30% amplitude); this should result in a suspension without any visible protein pellet left.

25) Pellet the protein by centrifugation (5 min, 18,400 g) and remove supernatant.

26) Add 250 µL urea buffer to each sample.

27) Resuspend pellet by thoroughly pipetting up and down with a yellow pipette tip (~10 times).

28) Snap freeze the samples and store the samples at -20 °C until required

Reduction, alkylation and avidin enrichment

29) Thaw the samples on ice.

30) Add 2.5 µL DTT stock, vortex, spin down briefly and incubate for 15 min at 65°C while shaking (600 rpm).

31) Let samples cool down to room temperature (at least 5 min).

32) Add 20 µL IAA solution, vortex and incubate for 30 min at room temperature in the dark.

33) Add 70 µL 10% SDS solution, vortex and incubate for 5 min at 65°C. Spin down shortly after the samples cool down to room temperature.

34) For 24 samples remove 1.2 mL avidin beads from a 50% slurry (50 µL per sample) and divide over four 15 mL tubes (300 µL per tube).

Note: Be sure to properly homogenize the slurry before pipetting.

35) Wash beads once with 10 mL PBS. Pellet beads by centrifugation (2 min, 2500 *g*) and remove the supernatant with a suction pump.

36) Homogenize the beads in 6 mL PBS per tube.

37) For 24 samples prepare 24 tubes (15 mL) with 2 mL PBS and 1 mL beads from step 36. Add each individual sample from step 33 to one of these tubes.

38) Incubate while rotating at low speed using an overhead shaker for at least 3 h at room temperature.

Wash beads

39) Pellet beads by centrifugation (2 min, 2500 *g*) and remove the supernatant.

Note: Be careful not to suck up the beads. Leave a little liquid above the beads.

40) Wash the beads once with 6 mL PBS/SDS, followed by three times with 6 mL PBS. Pellet beads by centrifugation (2 min, 2500 *g*) and remove the supernatant.

On-bead digestion

41) Add 250 µL OB-Dig buffer to the beads and transfer to a 1.5 mL low binding tube.

42) Add 1 µL trypsin solution per sample

43) Digest overnight at 37 °C with vigorous shaking (950 rpm).

LCMS sample preparation

44) Spin down shortly and add 12.5 µL formic acid per sample, briefly vortex and spin down.

45) Filter off the beads with a bio-spin column by centrifugation (2 min, 600 *g*) and collect the flow-through in a 2 mL tube.

46) Condition the stage tips, load the sample and wash the sample following this centrifugation scheme.

Note: Flow-through from conditioning, loading, and washing can be discarded. Elution should be done in a low binding tube. Centrifugation speed and duration are merely estimates. Solutions should have entirely run through without drying of the column

Conditioning 1	50 µL MeOH	7 min 650 g
Conditioning 2	50 µL Stage tip solution B	7 min 650 g
Conditioning 3	50 µL Stage tip solution A	7 min 650 g
Loading	Sample from step 45	15 min 750 g
Washing	100 µL Stage tip solution A	10 min 750 g
Switch to the low binding tube		
Elution	100 µL Stage tip solution B	10 min 750 g

47) Evaporate the solvent in a SpeedVac at 45°C for 3 hours.

The samples can be stored at -20°C until required.

48) Reconstitute sample in 50 µL of LC-MS sample solution.

49) Prepare a QC sample: pool 2 µL from each sample.

LC-MS analysis

50) Inject 5 µL of the sample onto the UPLC-IMS-MS system (see LC-MS Analysis).

LC-MS Analysis

The peptides were measured as described previously for the NanoACQUITY UPLC System coupled to SYNAPT G2-Si high definition mass spectrometer [17]. A trap-elute protocol, where 5 µL of the digest is loaded on a trap column (C_{18} 100 Å, 5 µM, 180 µM x 20 mm, Waters) followed by elution and separation on the analytical column (HSS-T3 C18 1.8 µM, 75 µM x 250 mm, Waters). The sample is brought onto this column at a flow rate of 10 µL/min with 99.5% solvent A for 2 min before switching to the analytical column. Peptide separation is achieved using a multistep concave gradient based on gradients previously described [30]. The column is re-equilibrated to initial conditions after washing with 90% solvent B. The rear seals of the pump are flushed every 30 min with 10% (vol/vol) ACN. [Glu1]-fibrinopeptide B (GluFib) is used as a lock mass compound. The auxiliary pump of the LC system is used to deliver this peptide to the reference sprayer (0.2 µL/min). A UDMSe method is set up as described in Distler et al. Briefly, the mass range is set from 50 to 2,000 Da with a scan time of 0.6 seconds in positive, resolution mode. The collision energy is set to 4 V in the trap cell for low-energy MS mode. For the elevated energy scan, the transfer cell collision energy is ramped using drift-time specific collision energies. The lock mass is sampled every 30 seconds. For raw data processing, PLGS (v3.0.3) was used. The MS^E identification workflow was performed with the parameters summarized in SI Table 1 to search the human proteome from Uniprot (uniprot-homo-sapiens-trypsin-reviewed-2016_08_29.fasta). For the MV4-11 experiments, the canonical sequence of FLT3 was replaced with the ITD sequence stated in the SI. Protein quantification was performed using ISOQuant (v1.5). The parameter settings used are summarized in SI Table 2.

Quantification and statistical analysis

All data analysis starting from the ISOQuant output has been performed in Python. The corresponding Jupyter notebook file with all the used functions is included in the Supporting Information. To calculate the Student's t-test the script depends on the RPy2 2.9.0 package. The following packages are optional for plotting and API queries Bokeh (0.12.10), chembl_webresource_client. Heatmaps were created with Microsoft Excel.

Probe targets were selected based on the following cut-offs:

i) 2-fold enrichment of quantification value from negative (vehicle treated) to positive control (1 µM XO44).

ii) Probability associated with a Student's t-test (two-tailed distribution; two-sample equal variance) < 0.05 testing positive control vs negative control samples.

iii) Benjamini–Hochberg correction with an FDR of 10%.

iv) Annotated as proteins transferring Phosphate containing groups in the Uniprot-database (EC number Filter "2.7.-.-"). Downloaded on 21-12-2017 (http://www.uniprot.org/uniprot/?query=reviewed:yes%20AND%20organism:%22Homo%20sapiens%20(Human)%20[9606]%22+ec:2.7.-.-).

Kinase inhibitor targets were selected as follows: kinases displaying > 50% reduction in probe labeling comparing inhibitor pre-treated sample with positive control (1 µM XO44) after subtraction of negative control signal (vehicle treated).

Supplementary Information

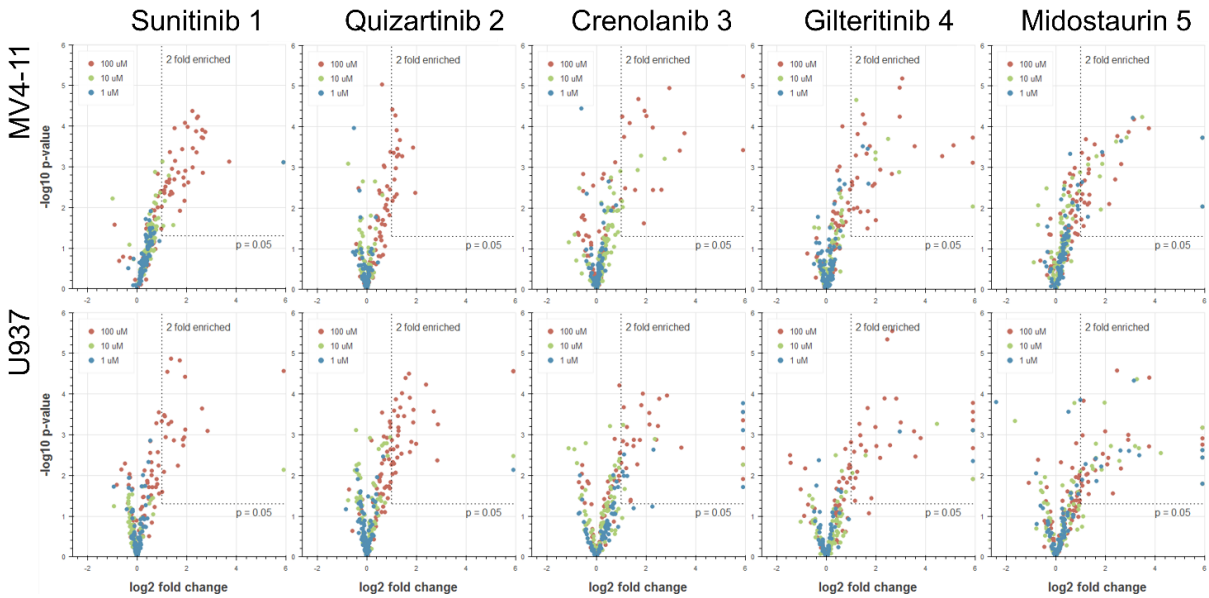

SI Figure 1: Competition with sunitinib, quizartinib, crenolanib, gilteritinib and midostaurin in living cells. Volcano plot of the label free quantification signal from IsoQuant for target kinases, pretreated with three different inhibitor concentrations in two cell lines. To enable plotting of all targets, infinite fold change (XO44 treated divided by competitor treated) was set to 60. A kinase was named a target if there was at least 50% reduction in quantification signal from probe treated samples vs inhibitor pretreated sample.

SI Table 1: The PLGS parameter settings used.

Parameter	**value**
Lock mass m/z	785.8426
Low energy threshold	150 counts
Elevated energy threshold	30 counts
Digest reagent	trypsin
Max missed cleavages	2
Modifications	Fixed carbamidomethyl C, variable oxidation M
FDR less than	1%
Fragments/peptide	2
Fragments/protein	5
Peptides/protein	1

SI Table 2: The ISOQuant parameter settings used.

parameter	**value**
isoquant.pluginQueue.name	design project and run ISOQuant analysis
process.peptide.deplete.PEP_FRAG_2	false
process.peptide.deplete.CURATED_0	false
process.peptide.statistics.doSequenceSearch	false
process.emrt.minIntensity	1000
process.emrt.minMass	500
process.emrt.rt.alignment.match.maxDeltaMass.ppm	10
process.emrt.rt.alignment.match.maxDeltaDriftTime	2
process.emrt.rt.alignment.normalizeReferenceTime	false
process.emrt.rt.alignment.maxProcesses	24
process.emrt.rt.alignment.referenceRun.selectionMethod	AUTO
process.emrt.clustering.preclustering.orderSequence	MTMTMT
process.emrt.clustering.preclustering.maxDistance.mass.ppm	6.06E-6
process.emrt.clustering.preclustering.maxDistance.time.min	0.202
process.emrt.clustering.preclustering.maxDistance.drift	2.02
process.emrt.clustering.distance.unit.mass.ppm	6.0E-6
process.emrt.clustering.distance.unit.time.min	0.2
process.emrt.clustering.distance.unit.drift.bin	2
process.emrt.clustering.dbscan.minNeighborCount	1
process.identification.peptide.minReplicationRate	2
process.identification.peptide.minScore	5.5
process.identification.peptide.minOverallMaxScore	5.5
process.identification.peptide.minSequenceLength	6
process.identification.peptide.acceptType.PEP_FRAG_1	true
process.identification.peptide.acceptType.IN_SOURCE	false
process.identification.peptide.acceptType.MISSING_CLEAVAGE	false
process.identification.peptide.acceptType.NEUTRAL_LOSS_H20	false
process.identification.peptide.acceptType.NEUTRAL_LOSS_NH3	false
process.identification.peptide.acceptType.PEP_FRAG_2	true
process.identification.peptide.acceptType.DDA	true
process.identification.peptide.acceptType.VAR_MOD	true

process.identification.peptide.acceptType.PTM	true
process.annotation.peptide.maxSequencesPerEMRTCluster	1
process.annotation.protein.resolveHomology	true
process.annotation.peptide.maxFDR	0.01
process.annotation.useSharedPeptides	all
process.normalization.lowess.bandwidth	0.3
process.normalization.orderSequence	XPIR
process.normalization.minIntensity	3000
process.quantification.peptide.minMaxScorePerCluster	5.5
process.quantification.peptide.acceptType.IN_SOURCE	false
process.quantification.peptide.acceptType.MISSING_CLEAVAGE	false
process.quantification.peptide.acceptType.NEUTRAL_LOSS_H20	false
process.quantification.peptide.acceptType.NEUTRAL_LOSS_NH3	false
process.quantification.peptide.acceptType.PEP_FRAG_1	true
process.quantification.peptide.acceptType.PEP_FRAG_2	false
process.quantification.peptide.acceptType.VAR_MOD	false
process.quantification.peptide.acceptType.PTM	false
process.quantification.peptide.acceptType.DDA	true
process.quantification.topx.degree	3
process.quantification.topx.allowDifferentPeptides	true
process.quantification.minPeptidesPerProtein	2
process.quantification.absolute.standard.entry	ENO1_YEAST
process.quantification.absolute.standard.fmol	50
process.quantification.topx.allowDifferentPeptides	true
process.quantification.absolute.standard.entry	ENO1_YEAST
process.quantification.absolute.standard.fmol	50
process.quantification.maxProteinFDR	0.01

Used Sequence FLT3-ITD in MV4-11:

>sp|F3LT00ITD1|FLT3_MV411 Receptor-type tyrosine-protein kinase FLT3 OS=Homo sapiens GN=FLT3_MV411 PE=1 SV=2
MPALARDGGQLPLLVVFSAMIFGTITNQDLPVIKCVLINHKNNDSSVGKSSSYPMVSESPEDLGCALRPQSSGTVYEAAAVEVDVS
ASITLQVLVDAPGNISCLWVFKHSSLNCQPHFDLQNRGVVSMVILKMTETQAGEYLLFIQSEATNYTILFTVSIRNTLLYTLRRPYF
RKMENQDALVCISESVPEPIVEWVLCDSQGESCKEESPAVVKKEEKVLHELFGTDIRCCARNELGRECTRLFTIDLNQTPQTTLPQ
LFLKVGEPLWIRCKAVHVNHGFGLTWELENKALEEGNYFEMSTYSTNRTMIRILFAFVSSVARNDTGYYTCSSSKHPSQSALVTI
VEKGFINATNSSEDYEIDQYEEFCFSVRFKAYPQIRCTWTFSRKSFPCEQKGLDNGYSISKFCNHKHQPGEYIFHAENDDAQFTK
MFTLNIRRKPQVLAEASASQASCFSDGYPLPSWTWKKCSDKSPNCTEEITEGVWNRKANRKVFGQWVSSSTLNMSEAIKGFLVK
CCAYNSLGTSCETILLNSPGPFPFIQDNISFYATIGVCLLFIVVLTLLICHKYKKQFRYESQLQMVQVTGSSDNEYFYVDFREYEYDH
VDFREYEYDLKWEFPRENLEFGKVLGSGAFGKVMNATAYGISKTGVSIQVAVKMLKEKADSSEREALMSELKMMTQLGSHENIV
NLLGACTLSGPIYLIFEYCCYGDLLNYLRSKREKFHRTWTEIFKEHNFSFYPTFQSHPNSSMPGSREVQIHPDSDQISGLHGNSFHS
EDEIEYENQKRLEEEEDLNVLTFEDLLCFAYQVAKGMEFLEFKSCVHRDLAARNVLVTHGKVVKICDFGLARDIMSDSNYVVRG
NARLPVKWMAPESLFEGIYTIKSDVWSYGILLWEIFSLGVNPYPGIPVDANFYKLIQNGFKMDQPFYATEEIYIIMQSCWAFDSRK
RPSFPNLTSFLGCQLADAEEAMYQNVDGRVSECPHTYQNRRPFSREMDLGLLSPQAQVEDS

References

(1) Fathi, A. T.; Chen, Y.-B. The Role of FLT3 Inhibitors in the Treatment of FLT3-Mutated Acute Myeloid Leukemia. *Eur. J. Haematol.* **2017**, *98* (4), 330–336.

(2) Griffith, J.; Black, J.; Faerman, C.; Swenson, L.; Wynn, M.; Lu, F.; Lippke, J.; Saxena, K. The Structural Basis for Autoinhibition of FLT3 by the Juxtamembrane Domain. *Mol. Cell* **2004**, *13* (2), 169–178.

(3) Lange, B.; Valtieri, M.; Santoli, D.; Caracciolo, D.; Mavilio, F.; Gemperlein, I.; Griffin, C.; Emanuel, B.; Finan, J.; Nowell, P. Growth Factor Requirements of Childhood Acute Leukemia: Establishment of GM-CSF-Dependent Cell Lines. *Blood* **1987**, *70* (1), 192–199.

(4) Stirewalt, D. L.; Radich, J. P. The Role of FLT3 in Haematopoietic Malignancies. *Nat. Rev. Cancer* **2003**, *3* (9), 650–665.

(5) Grunwald, M. R.; Levis, M. J. FLT3 Inhibitors for Acute Myeloid Leukemia: A Review of Their Efficacy and Mechanisms of Resistance. *Int. J. Hematol.* **2013**, *97* (6), 683–694.

(6) Fiedler, W.; Kayser, S.; Kebenko, M.; Janning, M.; Krauter, J.; Schittenhelm, M.; Götze, K.; Weber, D.; Göhring, G.; Teleanu, V.; et al. A Phase I/II Study of Sunitinib and Intensive Chemotherapy in Patients over 60 Years of Age with Acute Myeloid Leukaemia and Activating *FLT3* Mutations. *Br. J. Haematol.* **2015**, *169* (5), 694–700.

(7) Kayser, S.; Levis, M. J. Advances in Targeted Therapy for Acute Myeloid Leukaemia. *Br. J. Haematol.* **2018**, *180* (4), 484–500.

(8) Levis, M. Midostaurin Approved for FLT3-Mutated AML. *Blood* **2017**, *129* (26), 3403–3406.

(9) Stone, R. M.; Manley, P. W.; Larson, R. A.; Capdeville, R. Midostaurin: Its Odyssey from Discovery to Approval for Treating Acute Myeloid Leukemia and Advanced Systemic Mastocytosis. *Blood Adv.* **2018**, *2* (4), 444–453.

(10) Davis, M. I.; Hunt, J. P.; Herrgard, S.; Ciceri, P.; Wodicka, L. M.; Pallares, G.; Hocker, M.; Treiber, D. K.; Zarrinkar, P. P. Comprehensive Analysis of Kinase Inhibitor Selectivity. *Nat. Biotechnol.* **2011**, *29* (11), 1046–1051.

(11) Wodicka, L. M.; Ciceri, P.; Davis, M. I.; Hunt, J. P.; Floyd, M.; Salerno, S.; Hua, X. H.; Ford, J. M.; Armstrong, R. C.; Zarrinkar, P. P.; et al. Activation State-Dependent Binding of Small Molecule Kinase Inhibitors: Structural Insights from Biochemistry. *Chem. Biol.* **2010**, *17* (11), 1241–1249.

(12) Zhao, Q.; Ouyang, X.; Wan, X.; Gajiwala, K. S.; Kath, J. C.; Jones, L. H.; Burlingame, A. L.; Taunton, J. Broad-Spectrum Kinase Profiling in Live Cells with Lysine-Targeted Sulfonyl Fluoride Probes. *J. Am. Chem. Soc.* **2017**, *139* (2), 680–685.

(13) van Esbroeck, A. C. M.; Janssen, A. P. A.; Cognetta, A. B.; Ogasawara, D.; Shpak, G.; van der Kroeg, M.; Kantae, V.; Baggelaar, M. P.; de Vrij, F. M. S.; Deng, H.; et al. Activity-Based Protein Profiling Reveals off-Target Proteins of the FAAH Inhibitor BIA 10-2474. *Science* **2017**, *356* (6342), 1084–1087.

(14) Klaeger, S.; Heinzlmeir, S.; Wilhelm, M.; Polzer, H.; Vick, B.; Koenig, P. A.; Reinecke, M.;

Ruprecht, B.; Petzoldt, S.; Meng, C.; et al. The Target Landscape of Clinical Kinase Drugs. *Science (80-.).* **2017**, *358* (6367), eaan4368.

(15) Patricelli, M. P.; Szardenings, A. K.; Liyanage Marek; Nomanbhoy Tyzoon K.; Wu Min; Weissig Helge; Aban Arwin; Chun Doris; Tanner, S.; Kozarich, J. W. Functional Interrogation of the Kinome Using Nucleotide Acyl Phosphates. *Biochemistry* **2007**, *46* (2), 350–358.

(16) Shi, H.; Zhang, C.-J.; Chen, G. Y. J.; Yao, S. Q. Cell-Based Proteome Profiling of Potential Dasatinib Targets by Use of Affinity-Based Probes. *J. Am. Chem. Soc.* **2012**, *134* (6), 3001–3014.

(17) van Rooden, E. J.; Florea, B. I.; Deng, H.; Baggelaar, M. P.; van Esbroeck, A. C. M.; Zhou, J.; Overkleeft, H. S.; van der Stelt, M. Mapping in Vivo Target Interaction Profiles of Covalent Inhibitors Using Chemical Proteomics with Label-Free Quantification. *Nat. Protoc.* **2018**, *13* (4), 752–767.

(18) Kolb, H. C.; Sharpless, K. B. The Growing Impact of Click Chemistry on Drug Discovery. *Drug Discov. Today* **2003**, *8* (24), 1128–1137.

(19) Bento, A. P.; Gaulton, A.; Hersey, A.; Bellis, L. J.; Chambers, J.; Davies, M.; Krüger, F. A.; Light, Y.; Mak, L.; McGlinchey, S.; et al. The ChEMBL Bioactivity Database: An Update. *Nucleic Acids Res.* **2014**, *42* (D1), D1083–D1090.

(20) Savitski, M. M.; Reinhard, F. B. M.; Franken, H.; Werner, T.; Savitski, M. F.; Eberhard, D.; Martinez Molina, D.; Jafari, R.; Dovega, R. B.; Klaeger, S.; et al. Tracking Cancer Drugs in Living Cells by Thermal Profiling of the Proteome. *Science* **2014**, *346* (6205), 1255784.

(21) Vasta, J. D.; Corona, C. R.; Wilkinson, J.; Zimprich, C. A.; Hartnett, J. R.; Ingold, M. R.; Zimmerman, K.; Machleidt, T.; Kirkland, T. A.; Huwiler, K. G.; et al. Quantitative, Wide-Spectrum Kinase Profiling in Live Cells for Assessing the Effect of Cellular ATP on Target Engagement. *Cell Chem. Biol.* **2018**, *25* (2), 206–214.e11.

(22) Lanning, B. R.; Whitby, L. R.; Dix, M. M.; Douhan, J.; Gilbert, A. M.; Hett, E. C.; Johnson, T. O.; Joslyn, C.; Kath, J. C.; Niessen, S.; et al. A Road Map to Evaluate the Proteome-Wide Selectivity of Covalent Kinase Inhibitors. *Nat. Chem. Biol.* **2014**, *10* (9), 760–767.

(23) Papadatos, G.; Gaulton, A.; Hersey, A.; Overington, J. P. Activity, Assay and Target Data Curation and Quality in the ChEMBL Database. *J. Comput. Aided. Mol. Des.* **2015**, *29* (9), 885–896.

(24) Mori, M.; Kaneko, N.; Ueno, Y.; Yamada, M.; Tanaka, R.; Saito, R.; Shimada, I.; Mori, K.; Kuromitsu, S. Gilteritinib, a FLT3/AXL Inhibitor, Shows Antileukemic Activity in Mouse Models of FLT3 Mutated Acute Myeloid Leukemia. *Invest. New Drugs* **2017**, *35* (5), 556–565.

(25) Lagresle-Peyrou, C.; Six, E. M.; Picard, C.; Rieux-Laucat, F.; Michel, V.; Ditadi, A.; Chappedelaine, C. D.; Morillon, E.; Valensi, F.; Simon-Stoos, K. L.; et al. Human Adenylate Kinase 2 Deficiency Causes a Profound Hematopoietic Defect Associated with Sensorineural Deafness. *Nat. Genet.* **2009**, *41* (1), 106–111.

(26) Six, E.; Lagresle-Peyrou, C.; Susini, S.; De Chappedelaine, C.; Sigrist, N.; Sadek, H.; Chouteau, M.; Cagnard, N.; Fontenay, M.; Hermine, O.; et al. AK2 Deficiency

Compromises the Mitochondrial Energy Metabolism Required for Differentiation of Human Neutrophil and Lymphoid Lineages. *Cell Death Dis.* **2015**, *6* (8), e1856.

(27) Hartsink-Segers, S. A.; Zwaan, C. M.; Exalto, C.; Luijendijk, M. W. J.; Calvert, V. S.; Petricoin, E. F.; Evans, W. E.; Reinhardt, D.; de Haas, V.; Hedtjärn, M.; et al. Aurora Kinases in Childhood Acute Leukemia: The Promise of Aurora B as Therapeutic Target. *Leukemia* **2013**, *27* (3), 560–568.

(28) Hsu, Y. C.; Coumar, M. S.; Wang, W.-C.; Shiao, H.-Y.; Ke, Y.-Y.; Lin, W.-H.; Kuo, C.-C.; Chang, C.-W.; Kuo, F.-M.; Chen, P.-Y.; et al. Discovery of BPR1K871, a Quinazoline Based, Multi-Kinase Inhibitor for the Treatment of AML and Solid Tumors: Rational Design, Synthesis, in Vitro and in Vivo Evaluation. *Oncotarget* **2016**, *7* (52), 86239–86256.

(29) Quentmeier, H.; Reinhardt, J.; Zaborski, M.; Drexler, H. G. FLT3 Mutations in Acute Myeloid Leukemia Cell Lines. *Leukemia* **2003**, *17* (1), 120–124.

(30) Distler, U.; Kuharev, J.; Navarro, P.; Tenzer, S. Label-Free Quantification in Ion Mobility–enhanced Data-Independent Acquisition Proteomics. *Nat. Protoc.* **2016**, *11* (4), 795–812.